15. IJP 2019

by Jatmiko Endro Suseno

Submission date: 19-Feb-2020 08:47AM (UTC+0700)
Submission ID: 1259862895
File name: 15_IJP_2019.docx (455.79K)
Word count: 3061
Character count: 14766

A Study of the Corona Discharge Theory for Multipoint-Plane Configurations

***A Y Wardaya*[1,2]*, *M Nur*[1], *J E Suseno*[1]**

Abstract: This paper presents the numerical calculation of current-voltage (*I-V*) characteristics that were produced by a corona discharges plasma generator for a multipoint-plane configuration in air and; its comparison with the experimental results. The total number of needles in this configuration is $8 \times 4 = 32$ with the distance between the point-to-plane electrodes (denoted as *c*) as the variable. The *I-V* characteristic curve of the numerical calculation results matches that of the experimental results for cases with a large distance *c* (*c* = 3 and 4 cm), and it shows a large deviation for cases with a small distance *c* (*c* = 1 and 2 cm). Differences in the *I-V* characteristic curve between the experimental and numerical results are due to the symmetrical spread of the ion current from the point-to-plane electrodes, which is more pronounced for larger values of *c*.

Keywords: Plasma generator, multipoint-plane configuration, electric field, electric current, *I-V* characteristics.

PACS Nos.: 02.30.−f; 02.30.Em; 02.30.Ik; 02.30.Mv; 02.70.−c

1. Introduction

The corona discharge technique has been widely used for various research studies. Some of the papers on various electrode model configurations of corona discharges that try to obtain potential, voltage, or electric current characteristic values include the tip-plane configuration [1], thin bar-needle configuration [2], cylinder-wire-plate configuration [3], sub-millimeter electrode gap configuration [4], point-to-ring configuration [5], and multipoint-plane configuration [6]. However, this paper discusses the current-voltage characteristics from the experimental results. Some other research studies have calculated values related to corona discharges, among which are electrical potential distribution of pin-multi-ring concentric electrodes [7], electro-hydrodynamic and wind-ion direction produced

*Corresponding author, E-mail:asepyoyowardayafisika@gmail.com

by plasma discharge [8], ionic wind generation of needle-to-cylinder electrode model [9], ionic wind generation of multi electrode model [10], electro hydrodynamic force by a corona discharge [11].

There are also research studies that discuss the direct application of the corona discharge electrode configuration; cold large-diameter plasma jet of a triple electrode model [12], electric potential distribution of various electrode models [13], and laser-induced streamer corona discharge of a needle-to-plate electrode model [14].

This research is considered an extension of the work reported by Jaworek and Krupa [6] for the case of comparing the numerical calculation and experimental results of voltage and electric current characteristics generated by a corona discharge from plasma electrodes using a multipoint configuration. According to Sigmond [15], a large electric field generation along with a saturated current in the form of a corona discharge that, in turn, produces corona plasma is due to the sharp end of one of the electrodes; and the asymmetrical shape of both electrodes.

In this study, we use a model of a multipoint-plane configuration that consists of two perpendicular plates on one of which $m \times n$ number of needles is attached, as depicted in Fig. 1.

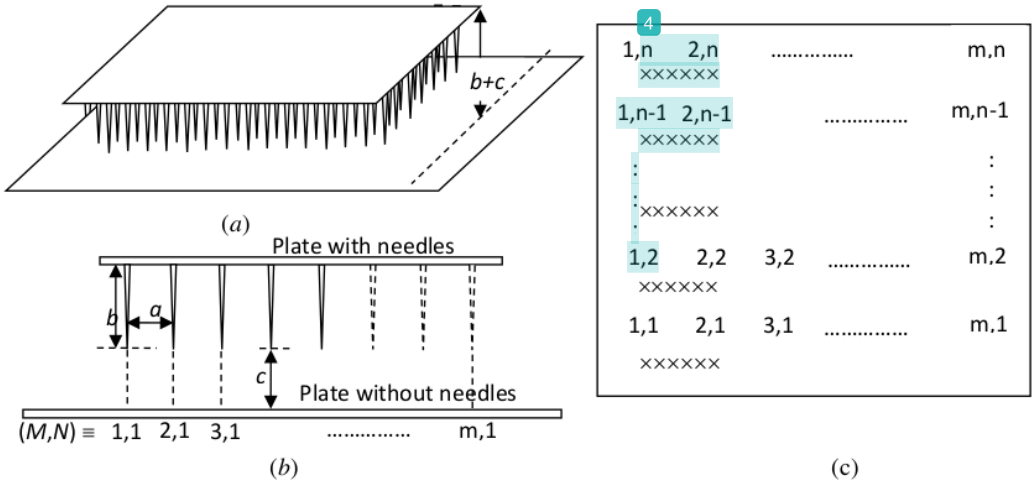

Figure 1. Model of the multipoint-plane configuration consisting of two parallel plates on one of which $m \times n$ needles are attached. The inter-needle distance is a, needle length is b, and distance between the point-to-plane electrodes is c. a). 3D representation of the electrode model. b). Side view of the electrode model. c). Top view of the location of $m \times n$ needles (marked ×).

As seen in Fig. 1, the needle length is b, inter-needle space is a, and distance between the point-to-plane electrodes is c. Hence, the distance between the two thin plates is $b + c$.The experiment of the corona discharge for the multipoint-plane configuration uses DC voltage;

with a positive polarity position at the point position and negative polarity at the plane position.

2. Electric Field Intensity

The electric field generated by the corona discharge from the point-plane configuration can be calculated using a formula [1] that transforms hyperbolic coordinates into Cartesian coordinates as follows,

$$E(x,y,z)=\frac{\left[V/\ln\left(\frac{z}{\varepsilon}\right)\right]}{\sqrt{c^2\cos^4\xi+x^2+y^2}}, \tag{1}$$

where the hyperbolic coordinates (η,ξ,ψ) relate to the 3D Cartesian coordinates as follows [1]:

$$x=-c\cos\xi\sinh\eta\sin\psi\,;\quad y=-c\cos\xi\sinh\eta\cos\psi\,;\quad z=c\sin\xi\cosh\eta\,, \tag{2}$$

where [1]

$$\cos^2\xi=\frac{u+\sqrt{u^2+4c^2\left(x^2+y^2\right)}}{2c^2}, \tag{3}$$

and [1]

$$u=c^2-\left(x^2+y^2+z^2\right)=c^2\cos^2\xi-\frac{\left(x^2+y^2\right)}{\cos^2\xi}, \tag{4}$$

and V is the input voltage.

To calculate certain positions on the plate without the needle against the needle tip position, we perform the calculation as if the upper part of Fig. 1.a only has one needle at position (2, 2) in Fig. 1.c. The position without a needle is designated as (•), whereas the position with a needle is assigned as (×), as shown in Fig. 2.a, for a 2D representation in the xz coordinates. However, seen from the z-axis, both position marks (•) and (×) for coordinate (2, 2) will coalesce as A_{00}. Therefore, a combination of those two marks in Fig. 2.b can simply be assigned as (×).

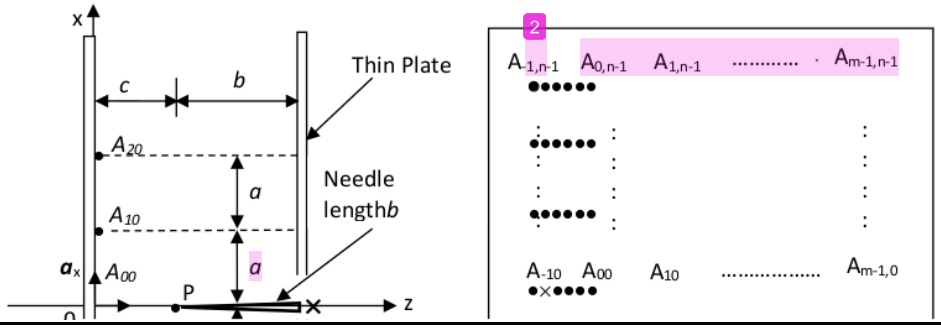

Figure2. a); Description of P points, A_{00}, A_{10}, A_{20} (marked •) on the 2D xz-plane (y = 0 and $z=\varsigma$, ς 1) that is induced by the electric current from the point-plane electrodes located in the positions marked (×). b); Full description of the points on the xy-plane from the z point of view without taking P into account; A_{-10}, A_{00}, A_{10}, etc. Observed from z, the position of A_{00} (•) coalesces with needle position (×), so that mark × is sufficient.

In Fig.2.a, a needle of length b (ending at point P), is attached on the plate (marked ×). The other points; (A_{00}, A_{10}, A_{20}, ...) are at a distance of $b+c$ from the plate with the needle, or points A_{00}, A_{10}, A_{20}, ...have a distance of $z=\varsigma\,;\varsigma$ 1 from the x-axis, where c is the distance from the needle tip to the plate without the needle.

The electric field generated by a needle electrode voltage source at point P with the coordinate $\xi=\frac{1}{2}\pi-\varepsilon$, where ε 1, and η = 0 (as x = y = 0, z~c, u~0), can be expressed similarly to equation [1]:

$$E_P = E\left(\xi=\tfrac{1}{2}\pi-\varepsilon,\eta=0\right)=\frac{\left[V/\ln\left(\frac{2}{\varepsilon}\right)\right]}{c\cos^2\left(\frac{1}{2}\pi-\varepsilon\right)}, \tag{5}$$

where the relationship of the coordinate η and variables x and y is defined as follows [1]:

$$\eta=\tanh^{-1}\left\{\frac{\sqrt{x^2+y^2}}{z}\tan\left(\tfrac{1}{2}\pi-\varepsilon\right)\right\}. \tag{6}$$

Equation (6) indicates a high electric field at the needle tip (point P); due to the value of $\cos^2\left(\frac{1}{2}\pi-\varepsilon\right)$ 1.

For the case at point A_{00} on the z-axis, with the distance c at the needle tip and its position at $z=\varsigma\,;\varsigma$ 1 ; $z\to 0$, the resulting electric field at point A_{00} at position x = y = 0 or $\eta=0$; is [1] as follows:

$$E_{00}\left(x=y=0,z\right)=\lim_{z\to 0}\frac{\left[cV/\ln\left(\frac{2}{\varepsilon}\right)\right]}{\left(c^2-z^2\right)}. \tag{7}$$

At another point $A_{\mu\nu}$ with $x = \mu a$ and $y = \nu a$; $\mu,\nu = 0, \pm1, \pm2,\ldots$, the electric field induced by a point-plane electrode voltage source with the needle coalescing with the z-axis and its point at point P; is as follows:

$$E_{\mu\nu}\left(x=\mu a,y=\nu a,z=\varsigma\right)=\frac{\left[2cV/\ln\left(\frac{2}{\varepsilon}\right)\right]}{\sqrt{{U_{\mu\nu}}^2+4\left(\mu^2+\nu^2\right)c^2a^2}}, \tag{8}$$

where

$$U_{\mu\nu}=2c^2\cos^2\xi=u_{\mu\nu}+\sqrt{{u_{\mu\nu}}^2+4c^2a^2\left(\mu^2+\nu^2\right)}\ , \tag{9}$$

and

$$u_{\mu\nu}=\lim_{z\to 0}\left[c^2-\left(x^2+y^2+z^2\right)\right]=\lim_{z\to 0}\left[c^2-\left(\mu^2+\nu^2\right)a^2-z^2\right]. \tag{10}$$

The following commutative relationship with absolute value applies;

$$E_{\mu\nu}=E_{\nu\mu}=E_{|\mu||\nu|};\ U_{\mu\nu}=U_{\nu\mu}=U_{|\mu||\nu|};\ u_{\mu\nu}=u_{\nu\mu}=u_{|\mu||\nu|}. \tag{11}$$

3. Electric Field Superposition

When there are $m\times n$ needle electrodes inducing a homogeneous electric field at certain points (Fig. 1.c), then the electric field inducing those points can be calculated using the concept of the electric field vector superposition that stems from those needles. In general, the magnitude of the electric field for points at $z = \zeta$, such as A_{00}, A_{20}, A_{14}, and so on. The calculation for the individual vector electric field where $x = \mu a$, $y = \nu a$ and $z = \zeta << 1$, is as follows:

$$\mathbf{E}_{\mu\nu}\left(x,y,z\right)=E_{\mu\nu}\left(\mu a,\nu a,\varsigma\right)\frac{\left\{x_N\mathbf{a}_x+y_N\mathbf{a}_y-c\mathbf{a}_z\right\}}{\sqrt{{x_N}^2+{y_N}^2+c^2}}, \tag{12}$$

where x_N, y_N and $z_N = -c$, which is the length of a 3D vector from the needle tip to certain positions (M, N) (Fig. 1.b). The electric field on the plate without a needle (plane xy) will be calculated (point A_{00} is always at distance c from the needle tip). The total electric field at point (M, N) is a superposition of the individual electric fields that consists of $A\times B$ needle electrodes that induce the point (M, N), with $m\times n$ being the total number of needles; hence, $A\times B \le m\times n$; can be written as follows:

$$\left(\mathbf{E}_T\right)_{\mathbf{MN}}=\sum_{\mu=0}^{A-1}\sum_{\nu=0}^{B-1}\mathbf{E}_{\mu\nu}\left(x,y,z\right),\qquad M=1,2,\ldots,m.\ \text{ and }\ N=1,2,\ldots,n. \tag{13}$$

Some indexing rules apply:

1. The index (M, N) is a fixed position index on the xy-plane that relates to the number of needles ($m \times n$).
2. The index μ, ν is the variable position index from point coordinate A_{ij} at position ($x = \mu a$, $y = \nu a$, $z = \zeta$) from the central coordinate (0, 0, 0) point of view, in which the reference point A_{00} is a position at distance c from the needle tip at the fixed index needle position (M, N).
3. The notations x_N, y_N and $z_N = -c$ are vector coordinates of the needle positions that stem from the needle tips and end at the points where the electric field is calculated on the plate without a needle (xy-plane).

The total electric field at certain positions (M, N) at distance c from the tip of the needles induced by the electric field generated by $A \times B$ needle electrodes (the total number of which is $m \times n$), based on equation (13) is as follows:

$$\left(\mathbf{E}_T\right)_{\mathbf{MN}} = \sum_{\mu=0}^{A-1}\sum_{\nu=0}^{B-1}\left[E_{|M-1-\mu|,|N-1-\nu|}\right]_{\mu+1,\nu+1}\frac{\left\{\left(M-1-\mu\right)a\mathbf{a}_x + \left(N-1-\nu\right)a\mathbf{a}_y - c\mathbf{a}_z\right\}}{\sqrt{\left(\left(M-1-\mu\right)a\right)^2 + \left(\left(N-1-\nu\right)a\right)^2 + c^2}}, \qquad (14)$$

where $M = 1, 2, 3, ..., m$ and $N = 1, 2, 3, ..., n$. This equation has electric field notation $E_{|M-1-\mu|,|N-1-\nu|}$ that which relates to equation (11).

We can consider that there is an arrangement of $m \times n$ needle electrodes as shown in Fig. 1.c. To calculate the electric field produced by each needle, at distance c from the needle tip, equation (14) is used. On the other hand, to calculate the total electric current produced by all needles, vector addition from each electric field unit in equation (14) must be performed. The total electric field resulting from all needles on the x- and y-axes will cancel each other out due to the symmetrical property, and what is left is the electric field components on the z-axis that will later be calculated.

Equation (14) describes the electric field resulting from the ions flow to the points at distances $x_\alpha = \alpha a$ and $y_\beta = \beta a$, with $\alpha = 0, 1, 2, \ldots, A\text{-}1$ and $\beta = 0, 1, 2, \ldots, B\text{-}1$, where A and B are the maximum points on the plate surface that exposed by the ion current at the x and y coordinates, respectively, in discrete numbers. These ion currents will flow from the needle tip to the plate surface with the maximum plate area of $xy = (A\text{-}1)(B\text{-}1)a^2$. Because the ion current flux has symmetrical, homogeneous, and continuous properties in the plane configuration, the discrete characteristics (summation form) in equation (14) become the

continuous characteristics (integration form) of the electric field quantity that can be solved using equation (15) ;

$$\left(E_z\right)_{m\times n}=\frac{c}{a^2}\sum_{\alpha=0}^{A-1}\sum_{\beta=0}^{B-1}\int_{x=0}^{a\alpha}dx_\alpha\int_{y=0}^{a\beta}dy_\beta\frac{\left[VK_{|\alpha\|\beta|}/\ln\left(\frac{2}{\varepsilon}\right)\right]}{\left(x_\alpha{}^2+y_\beta{}^2+c^2\right)}. \tag{15}$$

Substitution from 2D Cartesian coordinates to the polar coordinates results in the following:

$$\left(E_z\right)_{m\times n}=\frac{c}{a^2}\left[\frac{VK_{|\alpha\|\beta|}}{\ln\left(\frac{2}{\varepsilon}\right)}\right]\sum_{\alpha=0}^{A-1}\sum_{\beta=0}^{B-1}\int_{\rho=0}^{a\sqrt{\alpha^2+\beta^2}}\frac{\rho_{\alpha\beta}}{\left(\rho_{\alpha\beta}{}^2+c^2\right)}d\rho_{\alpha\beta}\int_{\phi=0}^{2\pi}d\phi,\quad \rho_{\alpha\beta}{}^2=x_\alpha{}^2+y_\beta{}^2, \tag{16}$$

and this generates the electric field given by the following:

$$\left(E_z\right)_{m\times n}=\frac{\pi c}{a^2}\left[\frac{V}{\ln\left(\frac{2}{\varepsilon}\right)}\right]\sum_{\alpha=0}^{A-1}\sum_{\beta=0}^{B-1}K_{|\alpha\|\beta|}\ln\left|\frac{a^2\left(\alpha^2+\beta^2\right)+c^2}{c^2}\right|. \tag{17}$$

4. Angle of Plasma Ion Flow

We note that not all points at positions $A_{\mu\nu}$;$\mu,\nu=0,\pm1,\pm2,\ldots$, can be induced by the electric field. According to Nur et al. [8], the angular deviation of the plasma ion flow from the point location induced by the electric field to the perpendicular direction of the needle is around 60°, up to a maximum of 67°, as shown in Fig. 3.

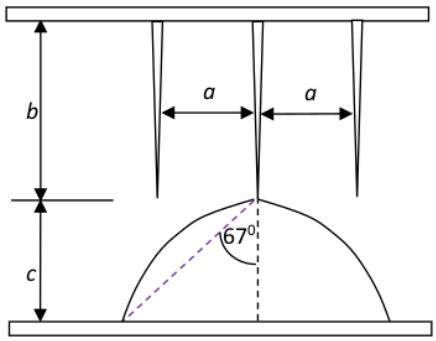

Figure 3. Maximum angular deviation of the electric field from the induced point location to the perpendicular direction of the needle is around 67°.

The relationship of θ and the position $A_{|\alpha||\beta|}$ can be calculated with the following equation:

$$\theta=\tan^{-1}\left\{\frac{a}{c}\sqrt{\alpha^2+\beta^2}\right\}\le 67^o,\ \text{at position } A_{|\alpha||\beta|}. \tag{18}$$

To verify the numerical simulations, we conducted an experiment to determine the relationship between the electric current I and voltage source V using a plasma discharge with

multipoint-plane configuration, which has been performed at the Radiation Physics Laboratory at Diponegoro University. The needles were arranged in an 8 × 4 = 32 needle formation with $a = 0.8068$ cm, $b = 0.018$ cm and c was varied at 1 cm ; 2 cm ; 3 cm and 4 cm. The overall value of $K_{\alpha\beta}$ for the 8 × 4 needle configuration is as follows:

$$K_{00} = 32 \; ; \; K_{|0||\beta|} = K_{|\alpha||0|} = 64 \text{ and } K_{|\alpha||\beta|} = 128 \text{ for } \alpha, \beta = 1, 2, \ldots, 7. \qquad (19)$$

The values of $A_{|\alpha||\beta|}$, index couple (α, β); and position number $K_{|\alpha||\beta|}$ for each variation of c, (taking equation (18) into account); are given in Table 1;

Table 1. Values of position $A_{|\alpha||\beta|}$, index couple (α, β), and position number $K_{|\alpha||\beta|}$ for varied c.

No.	c	Position	(α, β)	$K_{\|\alpha\|\|\beta\|}$
1.	1 cm	A_{00} , $A_{0\|\|1\|}$, $A_{1\|\|0\|}$, $A_{1\|\|1\|}$, $A_{1\|\|2\|}$, $A_{2\|\|1\|}$, $A_{2\|\|2\|}$	(0,0) ; (0,1) ; (1,0); (1,1) ; (1, 2) ; (2,1) ; (2, 2).	$K_{\|0\|\|0\|}$, $K_{\|0\|\|1\|}$, $K_{\|1\|\|0\|}$, $K_{\|1\|\|1\|}$, $K_{\|1\|\|2\|}$, $K_{\|2\|\|1\|}$, $K_{\|2\|\|2\|}$.
2.	2 cm	$A_{\|0\|\|0\|}$, … , $A_{\|3\|\|3\|}$, $A_{\|3\|\|4\|}$, $A_{\|3\|\|5\|}$, $A_{\|4\|\|3\|}$, $A_{\|5\|\|3\|}$.	(0,0) ; (0,1) ; (1,0) ; …. ; (3,3) ; (3, 4) ; (3,5) ; (4, 3) ; (5, 3).	$K_{\|0\|\|0\|}$, … , $K_{\|3\|\|3\|}$, $K_{\|3\|\|4\|}$, $K_{\|3\|\|5\|}$, $K_{\|4\|\|3\|}$, $K_{\|5\|\|3\|}$.
3.	3 cm	A_{00} , $A_{0\|\|1\|}$, $A_{1\|\|0\|}$, $A_{1\|\|1\|}$, …., $A_{\|6\|\|6\|}$, $A_{7\|\|6\|}$, $A_{\|6\|\|7\|}$	(0,0) ; (0,1) ; (1,0) ; …. ; (6,6) ; (7, 6) ; (6,7).	$K_{\|0\|\|0\|}$, $K_{\|0\|\|1\|}$, $K_{\|1\|\|0\|}$, … , $K_{\|6\|\|6\|}$, $K_{\|7\|\|6\|}$, $K_{\|6\|\|7\|}$.
4.	4 cm	A_{00} , $A_{0\|\|1\|}$, $A_{1\|\|0\|}$, $A_{1\|\|1\|}$, …., $A_{\|7\|\|6\|}$, $A_{\|6\|\|7\|}$, $A_{7\|\|7\|}$	(0,0) ; (0,1) ; (1,0) ; …. ; (6,6) ; (7, 6) ; (6,7) ; (7,7).	$K_{\|0\|\|0\|}$, $K_{\|0\|\|1\|}$, $K_{\|1\|\|0\|}$, … , $K_{\|6\|\|6\|}$, $K_{\|7\|\|6\|}$, $K_{\|6\|\|7\|}$, $K_{\|7\|\|7\|}$.

5. Induced Current

In the case of the point-plane configuration, the charge Q induced on the plane electrode becomes [1] the following;

$$Q = \frac{V(\xi) - V}{V} q, \qquad (20)$$

where V is the potential of the point electrode and q is the charge of the electric flux lines coming from the multipoint to the plane configuration as defined in equation (20), and the induced current yields the following:

$$i = -\frac{dQ}{dt} = -\frac{q}{V}\frac{dV(\xi)}{ds}\frac{ds}{dt} = \mu_0 \frac{q}{V} E^2. \qquad (21)$$

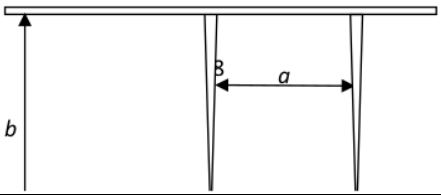

Figure 4. Electric field calculation on the plane electrode (B) positioned at distance c from the point electrode (A).

According to Halliday et al.[16], the electric field strength at point B can be written as follows:

$$E_Q = \frac{q}{4\pi\varepsilon_0 c}\frac{1}{(b+c)} \quad . \tag{22}$$

When the results from the work by Coelho and Debeau [1] are used as a comparison, the electric field strength at B located at distance c from the point electrode can be written as follows:

$$E_Q \cong \frac{V}{c\ln\left(\frac{2}{\epsilon}\right)} \quad . \tag{23}$$

Using equations (22) and (23), charge q is yielded as follows:

$$q = \frac{4\pi\varepsilon_0 (b+c)V}{\ln\left(\frac{2}{\epsilon}\right)} \quad . \tag{24}$$

The electric current from the multipoint-plane configuration with 32 needles (N = 32) can be calculated using the equations (17), (21), and (24) as follows:

$$i = -N\frac{dQ}{dt}$$

$$= \mu_0 N \frac{4\pi^3\varepsilon_0 (b+c)c^2V^2}{a^4\ln^3\left(\frac{2}{\epsilon}\right)}\left\{\sum_{\alpha=0}^{A-1}\sum_{\beta=0}^{B-1} K_{|\alpha||\beta|}\ln\left|\frac{a^2(\alpha^2+\beta^2)+c^2}{c^2}\right|\right\}^2 \quad \text{with} \quad \epsilon <<< 1, \tag{25}$$

where μ_0 and ε_0 are the mobility ($4\pi \times 10^{-7}$ Wb/A.m) and permittivity ($8{,}85 \times 10^{-12}$ F/m) at the vacuum space, respectively.

6. Results and Discussion

In the simulation graphs for the electric current I and voltage V, we use Table 1 and equation (25) for different values of c (1, 2, 3 and 4 cm). These simulation graphs are compared with experiment graphs of the same variations ofelectric current I and voltage V ;

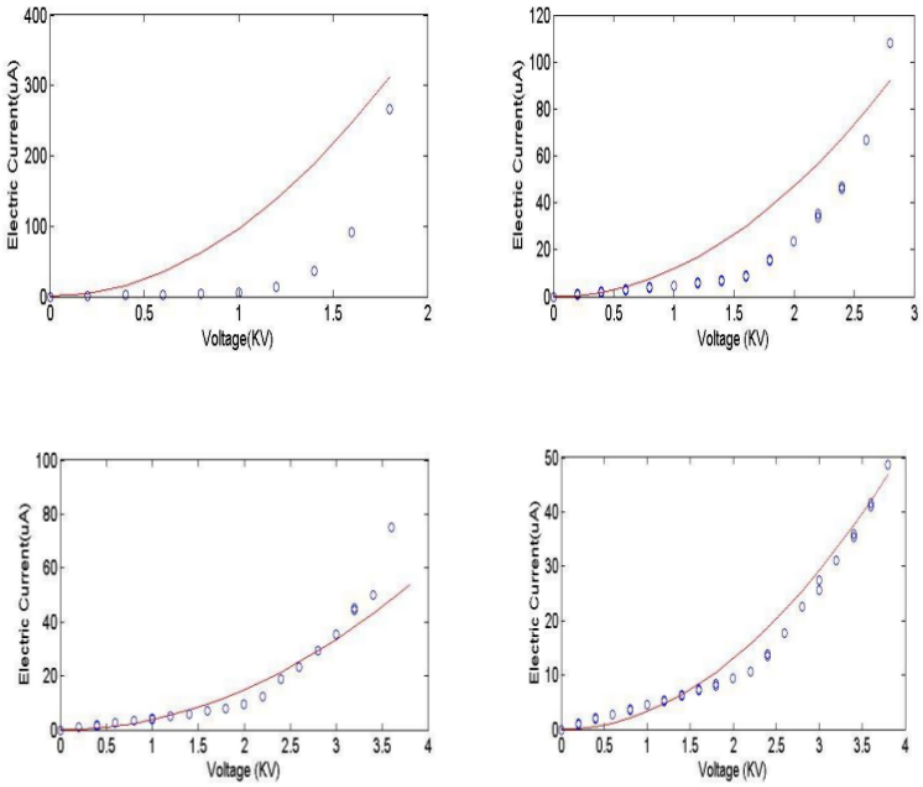

Figure 5. Graphs of the relationship between the electric current I and voltage source V obtained from the 8 × 4 = 32 needle electrode configuration, limited to 67° for the maximum deviation angle for$a$ = 0,8068 cm, b= 0.018 cm, and varied c at 1; 2; 3 and 4 cm. Blue circles indicate the experiment results. Red lines show simulation results from equation (25).

A theory of corona discharge with multipoint-plane configuration has been discussed. The calculations of the electric field and saturated current generated from this configuration when input voltage V is applied have also been elaborated. The calculation of the total electric field resulting from $m \times n$ needle electrodes must be done using the concept of the electric field vector superposition. This research employs an arrangement of 8×4 needle electrodes with varied distances between the point-to-plane electrodes (c) at 1, 2, 3, and 4 cm.

The resulting graphs show that the simulation results are closer to the experiment results when the distance c is larger, especially for c at 3 cm and 4 cm. A narrower c causes an asymmetrical and inhomogeneous ion flow in which some areas are flooded with more ions than predicted. For a higher$c$, the symmetrical and homogeneous ion flow is closer to the experimental results. This causes an electric current reading that is closer to the expected value. Moreover, a narrower c does not allow the maximum electric field deviation angle from the induced point location to the perpendicular needle position, which may reach 67°, while greater $c$allows this to take place, hence, almost all ion flow that stems from the needle electrodes reaches all the designated points on the plane without the needles, and in turn, yields a greater electric field. Another influencing factor for the electric current reading is the shape of the needle with a sharpness no closer than 0°, which is the ideal condition for electric field calculation.

These statements can be explained as follows, Equation (14) shows the 3D vector of the ion current flow model that flows from the needle tip to the bottom plate with a parabolic shape as shown in Fig. 3. To simplify equation (14), we assume that the ion current flows symmetrically so that the flowing 3D vector will be changed to one direction in the upright axis (z-axis) because the ion current direction at the xy-plane will be a symmetrical circle; therefore, it will eliminate the others. Another assumption is that the ion current in the direction of the z-axis will be homogenously distributed and close to continuously flowing, so that the vector and discrete (summation) characteristics in equation (14) are changed to continuous (integration) and scalar characteristics (only in the direction of the z-axis) in equation (15), where equation (15) is part of equation (25). Therefore, the conditions of homogenous continuity and symmetry will be better for an increased distance from the multipoint-plane to the bottom plate surface, so that the mathematical simulation will match the results of the experiment at a greater value of c.

7. Conclusion

The current-voltage (I-V) characteristics that were produced by the corona discharge plasma generator for the multipoint-plane configuration in the air could demonstrate the performance of a device. The total electric field inducing these points could be calculated using the concept of the electric field vector superposition that stems from these needles. The total number of needles in this configuration is $8 \times 4 = 32$, and there is a variation of distance

c, which is the distance between the point-to-plane electrodes. The between the numerical simulation and experimental results indicated that the *I-V* characteristic curve is simulated better for longer distances between the point-to-plane electrodes, which is roughly longer than 3 cm; due to better symmetry and homogeneity of the ion current flows from the multipoint-plane to the plane configuration.

15. IJP 2019

ORIGINALITY REPORT

3%	3%	1%	1%
SIMILARITY INDEX	INTERNET SOURCES	PUBLICATIONS	STUDENT PAPERS

PRIMARY SOURCES

1	scala.uc3m.es Internet Source	<1%
2	zapdoc.tips Internet Source	<1%
3	bug.cf1.ru Internet Source	<1%
4	www.ece.uvic.ca Internet Source	<1%
5	Wang, W.. "The orbital interaction of adsorbed CO on NiO (001;111) surface: A periodic density functional theory study", Applied Surface Science, 20060215 Publication	<1%
6	www.lasercenter.pl Internet Source	<1%
7	orbi.uliege.be Internet Source	<1%
8	www.science.gov Internet Source	<1%

9	cache.freescale.com Internet Source	<1%
10	Submitted to Mersin Ãniversitesi Student Paper	<1%
11	slideheaven.com Internet Source	<1%
12	Edwin Román-Hernández, José Guadalupe Santiago-Santiago, Gilberto Silva-Ortigoza, Ramón Silva-Ortigoza. "Wavefronts and caustic of a spherical wave reflected by an arbitrary smooth surface", Journal of the Optical Society of America A, 2009 Publication	<1%

Exclude quotes	Off	Exclude matches	Off
Exclude bibliography	Off		